Electronic Supplementary Material (ESI) for Journal of Materials Chemistry A.

Bonding dependent lithium storage behaviors of molybdenum oxides for next-generation Li-ion batteries

Hyunwoo Kim,[a] Chang-Dae Lee,[b] Dong In Kim,[a] Woosung Choi,[a] Dong-Hwa Seo,[b] Won-Sub Yoon[a,*]

[a] *Department of Energy Science, Sungkyunkwan University, Suwon 16419, Republic of Korea*

[b] *School of Energy and Chemical Engineering, Ulsan National Institute of Science and Technology, Ulsan, 44919 Republic of Korea*

*** Corresponding author:**

E-mail: wsyoon@skku.edu; Postal Address: Prof. Won-Sub Yoon, Department of Energy Science, Sungkyunkwan University. Natural Sciences Campus, 2066, Seobu-ro, Jangan-gu, Suwon-si, Gyeonggi-do, Korea (16419)

Supplementary Discussion

Capacity contribution from each component in MoO_x/rGO composite

Based on the TGA result, the weight ratio of rGO in MoO_2/rGO and MoO_3/rGO is ~19.1% and ~23.1%, respectively. The reversible capacity of ~1017 mAh g^{-1} in MoO_2/rGO and ~1110 mAh g^{-1} in MoO_3/rGO can be expressed as below.

$\rightarrow$ $0.191\ \alpha + 0.809\ \beta = \sim 1017$ mAh g^{-1} (MoO_2/rGO)

$\rightarrow$ $0.231\ \alpha + 0.769\ \gamma = \sim 1110$ mAh g^{-1} (MoO_3/rGO)

α: Specific reversible capacity from rGO

β, γ: Specific reversible capacity from MoO_2 and MoO_3 in the composites

The theoretical maximum capacity of rGO (α) is ~744 mAh g^{-1} ($C_6 + 2Li^+ + 2\ e^- = Li_2C_6$), based on lithium ion accommodation on the both sides of each graphene monolayers.[1–3]

$\rightarrow$ $\beta = 1081$ mAh g^{-1}, $\gamma = 1099$ mAh g^{-1}.

Therefore, the specific capacity contribution of MoO_2 in MoO_2/rGO is 1081 mAh g^{-1}, and that of MoO_3 is 1099 mAh g^{-1}.

Kinetic investigation using cyclic voltammetry

The relationship between current (i) and scan rate (v) obeys the following power laws,[4,5] where a and b are variable constants.

$$i = av^b \quad (1)$$

Thus, the b value can be obtained by calculating the slope of the log(*i*) versus log(*v*) curves.

$$\log i = b \log v + \log a \quad (2)$$

The b-value is between 0.5 and 1.0, which approaches 0.5 for a diffusion-controlled process and 1.0 for a capacitive reaction.

To obtain b-value at the redox potential, the CV curves of MoO_x/rGO composite were recorded with scan rates from 0.1–0.5 mV s^{-1}, as shown in **Fig. S4**.

Supplementary Tables

Table S1. Curves fitting results of Li 1s and O 1s XPS spectra of fully lithiated MoO_3/rGO and MoO_2/rGO electrodes after etching the surface

Spectra	Component	Position (eV)	FWHM (eV)	Area (%)
MoO_2/rGO Li 1s XPS	LiF	56.4	1.273	2.8
	Li_2CO_3	55.3	1.544	16.9
	Li_xMoO_2	54.4	2.404	60.8
	Li_2O	53.7	2.003	10.2
	Metallic Li	52.3	1.406	9.3
MoO_3/rGO Li 1s XPS	LiF	56.4	1.273	4.1
	Li_2CO_3	55.3	1.544	60.0
	Li_2O	53.7	2.003	35.9
MoO_2/rGO O 1s XPS	Li_2CO_3	532.0	2.079	46.5
	Li_xMoO_2	530.8	2.087	37.9
	Li_2O	528.5	1.480	15.6
MoO_3/rGO O 1s XPS	Li_2CO_3	532.0	2.079	66.9
	Li_2O	528.5	1.480	33.1

Supplementary Figures

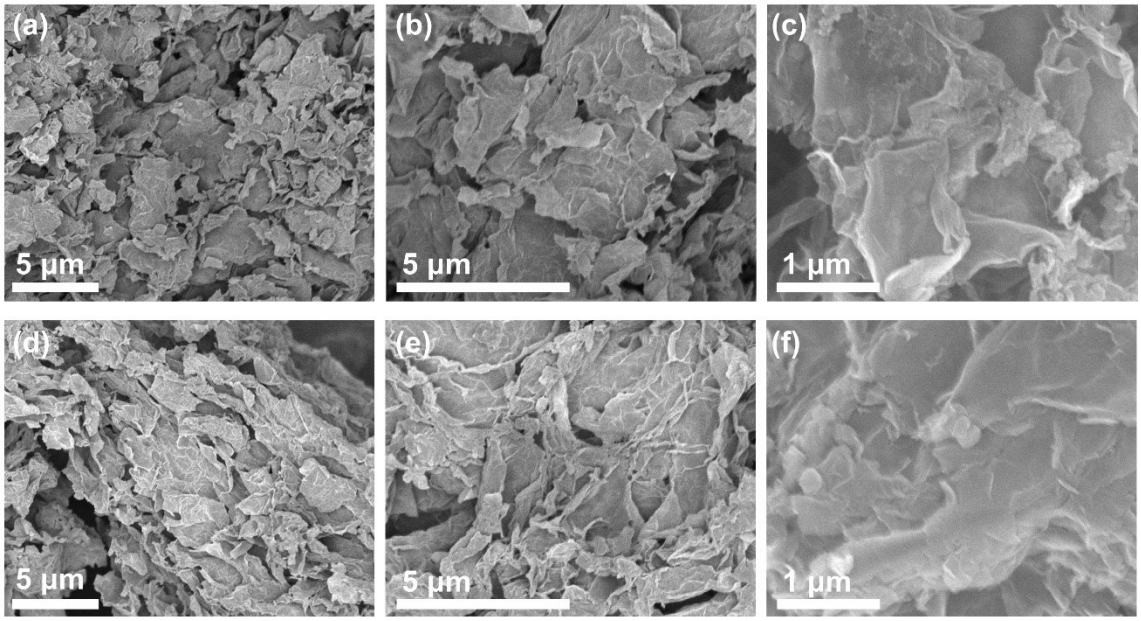

Fig. S1. SEM images of (a)–(c) MoO_2/rGO and (d)–(f) MoO_3/rGO with different magnifications.

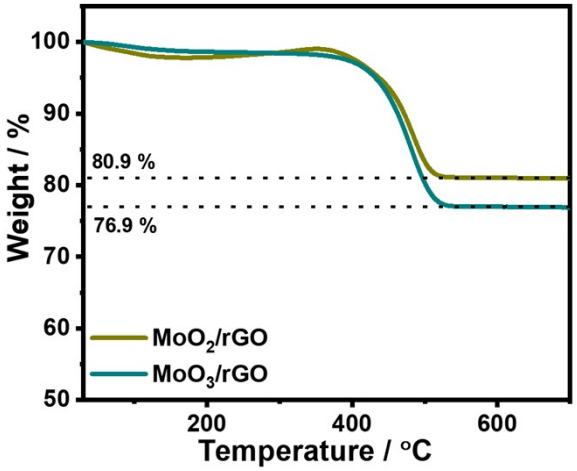

Fig. S2. TGA results of MoO_2/rGO and MoO_3/rGO.

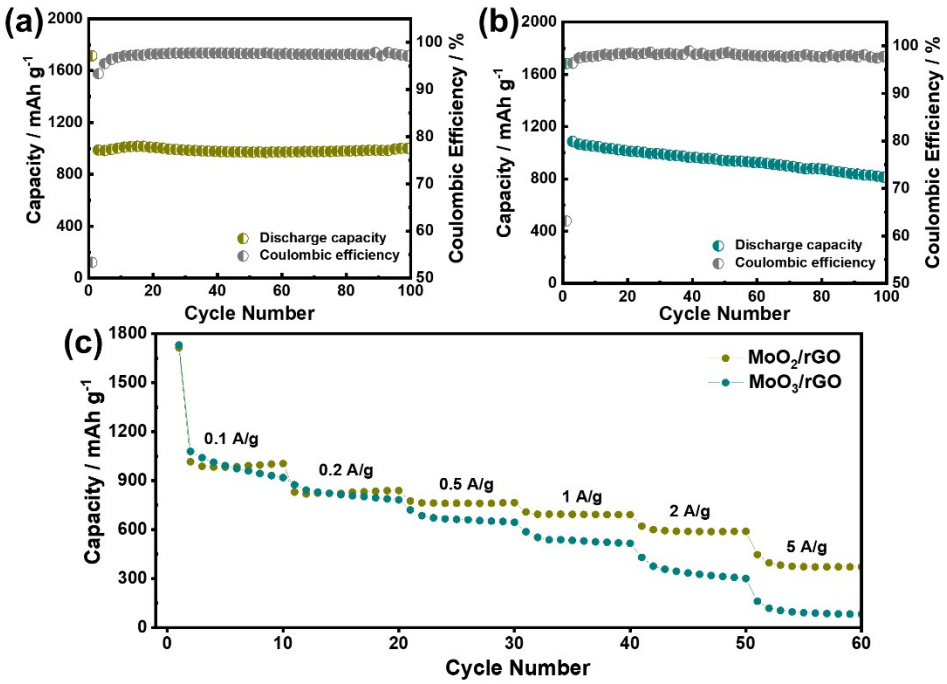

Fig. S3. Cycle performance test of (a) MoO_2/rGO and (b) MoO_3/rGO during 100 cycles under a specific current of 100 mA g^{-1}. (c) Rate capability of MoO_2/rGO and MoO_3/rGO.

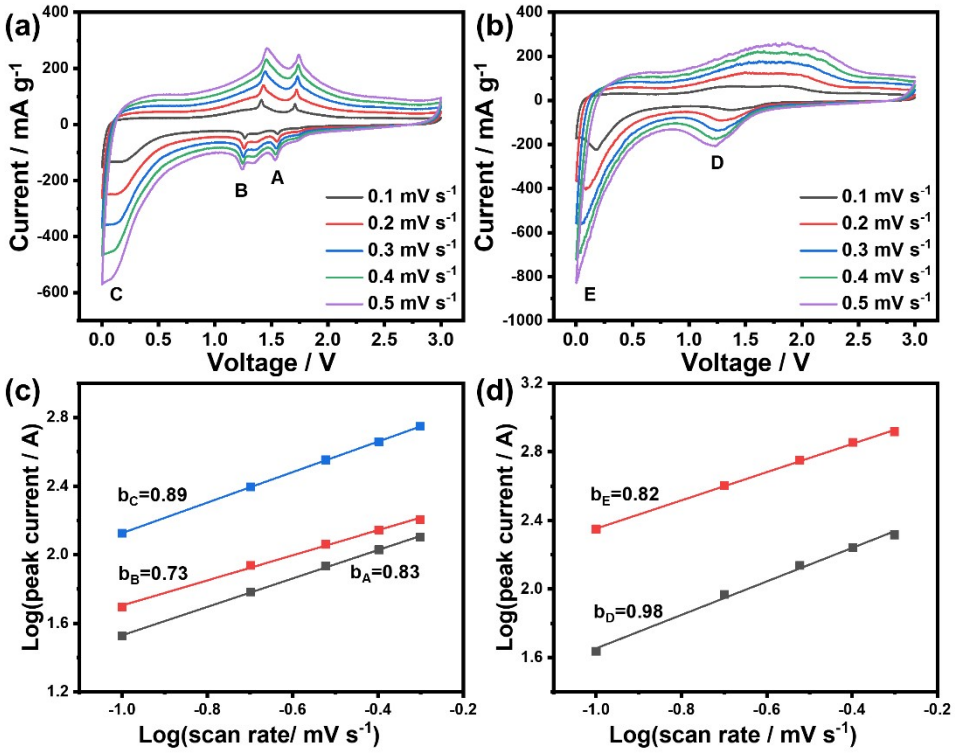

Fig. S4. CV curves of (a) MoO_2/rGO and (b) MoO_3/rGO with scan rate increasing from 0.1 to 0.5 mV s^{-1}. Relation between log(peak current) and log(scan rate) of (c) MoO_2/rGO and (d) MoO_3/rGO.

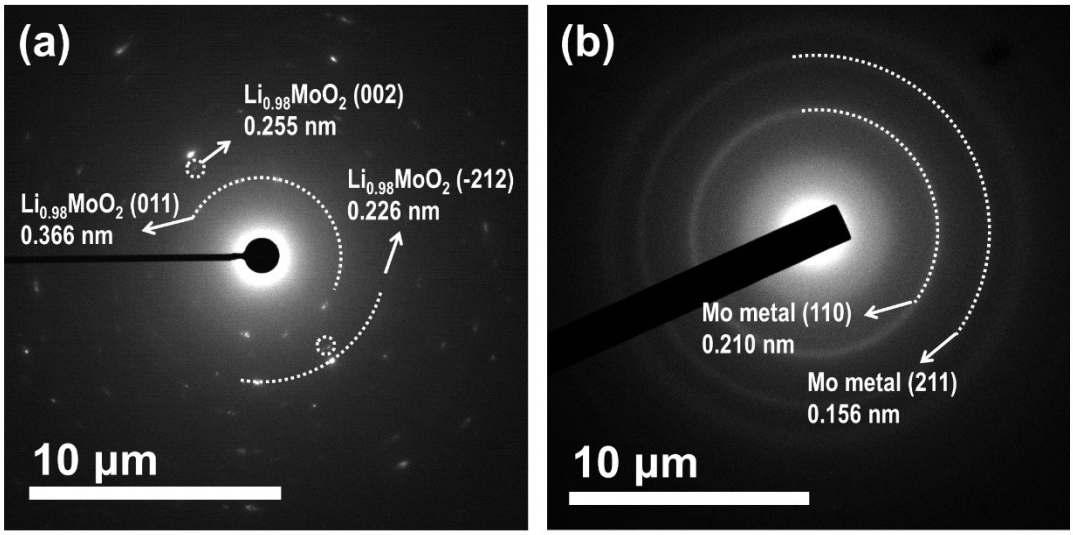

Fig. S5. SAED pattern of (a) MoO_2/rGO and (b) MoO_3/rGO electrodes after full discharge.

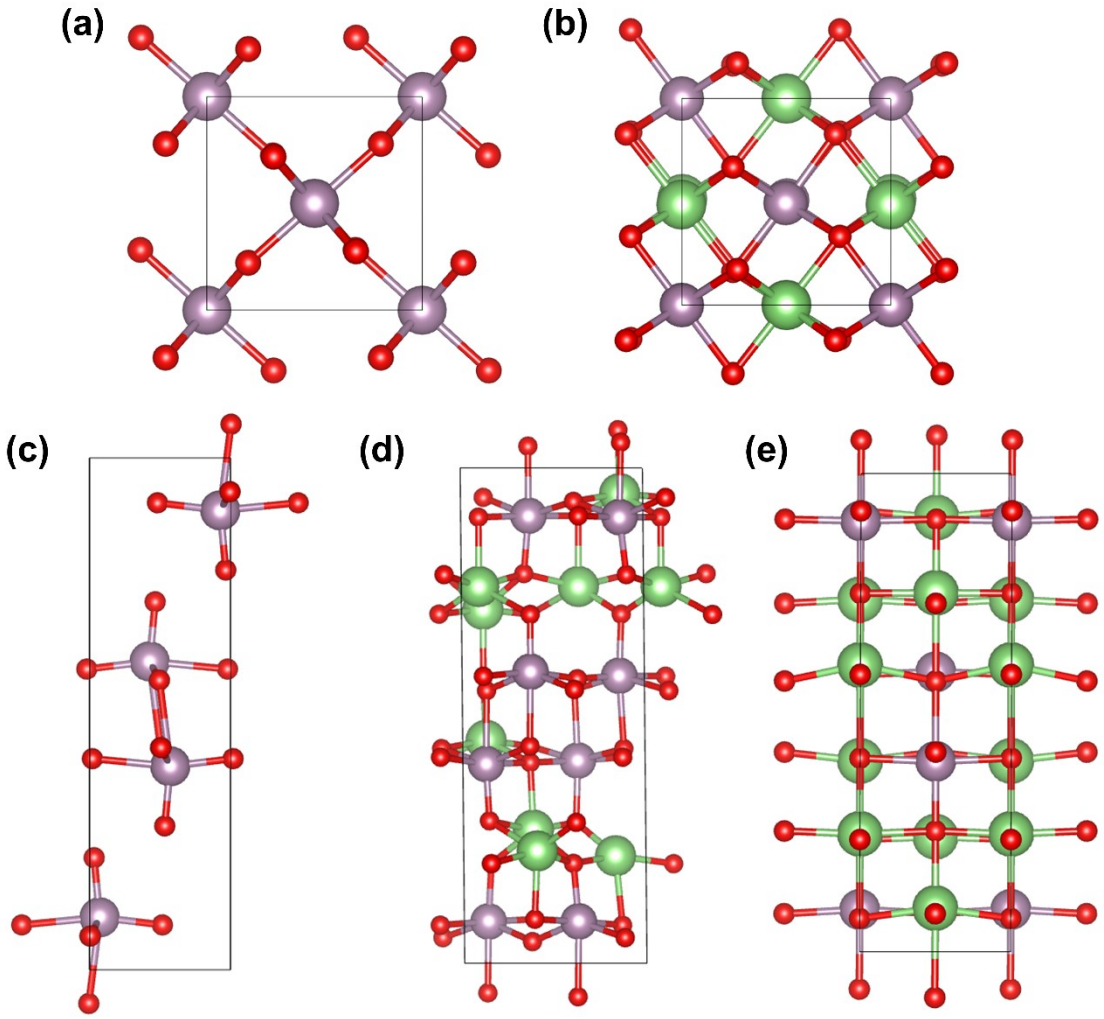

Fig. S6. Crystal structural models for calculating Mo–O bonding characteristics in (a) MoO_2, (b) $LiMoO_2$, (c) MoO_3, (d) $LiMoO_3$, and (e) Li_2MoO_3.

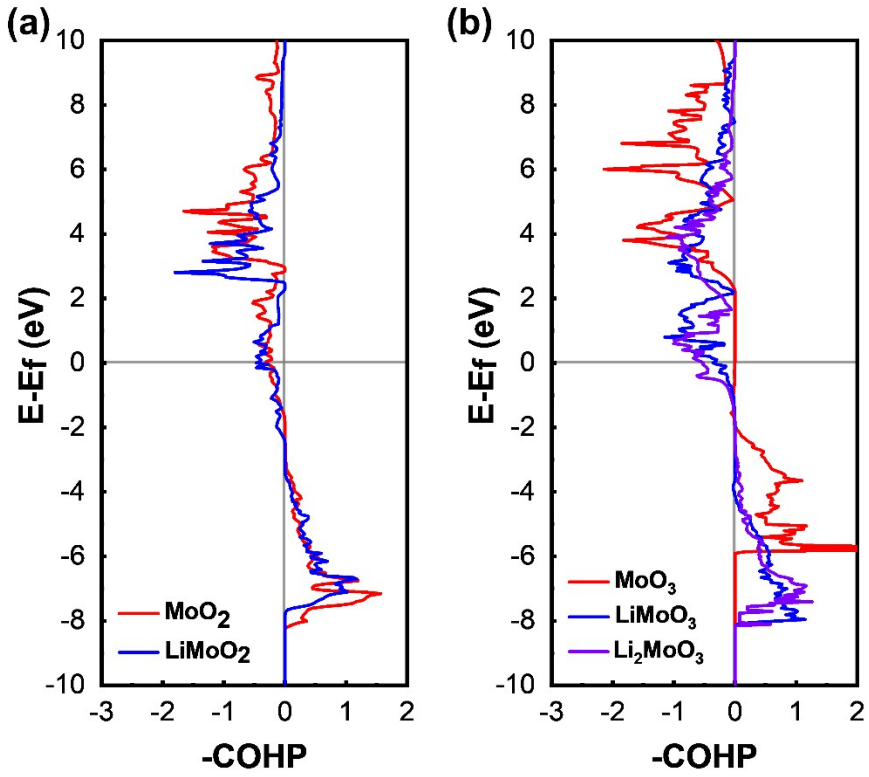

Fig. S7. COHP plots of (a) Li_xMoO_2 (x = 0, 1) and (b) Li_xMoO_3 (x = 0, 1, 2).

References

1 J.R. Dahn, T. Zheng, Y. Liu, J.S. Xue, *Science*, **1995**, *270*, 590–593.

2 G. Wang, B. Wang, X. Wang, J. Park, S. Dou, H. Ahn, K. Kim, *J. Mater. Chem.*, **2009**, *19*, 8378–8384.

3 R. Raccichini, A. Varzi, S. Passerini, B. Scrosati, *Nat. Mater.*, **2015**, *14*, 271–279.

4 H. Lindström, S. Södergren, A. Solbrand, H. Rensmo, J. Hjelm, A. Hagfeldt, S.-E. Lindquist, *J. Phys. Chem. B*, **1997**, *101*, 7717–7722.

5 H.-E. Wang, X. Zhao, K. Yin, Y. Li, L. Chen, X. Yang, W. Zhang, B.-L. Su, G. Cao, *ACS Appl. Mater. Interfaces*, **2017**, *9*, 43665–43673.